

PUBLICATION V

# **Determination of matrix diffusion properties of granite**

In: Mater. Res. Soc. Symp. Proc.  
Vol. 985, 6 p.

Copyright 2007 Materials Research Society.  
Reprinted with permission from the publisher.



## Determination of Matrix Diffusion Properties of Granite

Pirkko Holttä<sup>1</sup>, Marja Siitari-Kauppi<sup>1</sup>, Nina Huittinen<sup>1</sup>, and Antti Poteri<sup>2</sup>

<sup>1</sup>Laboratory of Radiochemistry, P.O. Box 55, University of Helsinki, FI-00014, Finland

<sup>2</sup>VTT Processes, P.O. Box 1608, VTT, FI-02044, Finland

### ABSTRACT

Rock–core column experiments were introduced to estimate the diffusion and sorption properties of Kuru Grey granite used in block–scale experiments. The objective was to examine the processes causing retention in solute transport through rock fractures, especially matrix diffusion. The objective was also to estimate the importance of retention processes during transport in different scales and flow conditions. Rock–core columns were constructed from cores drilled into the fracture and were placed inside tubes to form flow channels in the 0.5 mm gap between the cores and the tube walls. Tracer experiments were performed using uranine, HTO, <sup>36</sup>Cl, <sup>131</sup>I, <sup>22</sup>Na and <sup>85</sup>Sr at flow rates of 1–50  $\mu\text{L}\cdot\text{min}^{-1}$ . Rock matrix was characterized using <sup>14</sup>C–PMMA method, scanning electron microscopy (SEM), energy dispersive X–ray micro analysis (EDX) and the B.E.T. method.

Solute mass flux through a column was modelled by applying the assumption of a linear velocity profile and molecular diffusion. Coupling of the advection and diffusion processes was based on the model of generalised Taylor dispersion in the linear velocity profile. Experiments could be modelled applying a consistent parameterization and transport processes. The results provide evidence that it is possible to investigate matrix diffusion at the laboratory scale. The effects of matrix diffusion were demonstrated on the slightly–sorbing tracer breakthrough curves. Based on scoping calculations matrix diffusion begins to be clearly observable for non–sorbing tracer when the flow rate is 0.1  $\mu\text{L}\cdot\text{min}^{-1}$ . The experimental results presented here cannot be transferred directly to the spatial and temporal scales that prevail in an underground repository. However, the knowledge and understanding of transport and retention processes gained from this study is transferable to different scales from laboratory to in–situ conditions.

### INTRODUCTION

Crystalline rock is being considered as a host medium for the repository of highly radioactive spent nuclear fuel in Finland and elsewhere. The geosphere would act as the ultimate barrier retarding the migration of radionuclides to the biosphere if radionuclides were to be released through engineered barriers. In crystalline rock water flows through a fracture network and radionuclide transport is thought to proceed along water–carrying fractures. Retardation occurs both in the fractures and within the rock matrix. The experimental column method used in this study was a direct approach for determining the parameters affecting the fracture flow described in radionuclide transport models. Radionuclide transport has been studied in the Finnish program earlier using flow–through fracture and crushed rock columns [1, 2]. Fracture flow and radionuclide transport have been studied in block–scale experiments using Kuru Grey granite [3–5]. The objectives of those studies were to examine the processes causing retention in solute transport through rock fractures, especially matrix diffusion. The results can be used to estimate importance of retention processes during transport in different scales and flow conditions. Rock–core column experiments

were introduced to estimate the diffusion and sorption properties of Kuru Grey granite used in block-scale experiments. The results of this work will be used to estimate radionuclide transport times and retardation parameters in artificial fractures before conducting block-scale experiments in natural fracture. We describe below the rock matrix characterization and the experimental design utilising rock-core columns as well as present tracer test results and scoping calculations.

## ROCK MATRIX CHARACTERIZATION

Kuru Grey granite was obtained from Kuru Quarry, Tampereen Kovakivi Oy, Finland. The total porosity and the surface areas of mineral grains available for sorption and migration of species were determined by the  $^{14}\text{C}$ -PMMA method [6, 7]. Pore apertures and geometry in the mineral phases were analyzed by scanning electron microscopy (SEM), and the minerals and sorbed tracer were quantified by energy dispersive X-ray microanalysis (EDX). The specific surface area of the solid rock was determined by the B.E.T. Hg impregnation method. Kuru Grey granite is fine-grained, non-foliated and equigranular with composition of 36% potassium feldspar, 35% quartz, 21% plagioclase and 8% amphibole and micas. Its density given by Tampereen Kovakivi Oy is  $2660 \text{ kg}\cdot\text{m}^{-3}$ . The total bulk porosity determined by water gravimetry and  $^{14}\text{C}$ -PMMA method was 0.4 %. The average grain size determined by SEM was 0.5–1.5 mm. The specific surface area was  $0.03 \text{ m}^2\cdot\text{g}^{-1}$  and the average pore diameter was 300–400 nm. A photo image of Kuru Grey granite and corresponding  $^{14}\text{C}$ -PMMA autoradiograph showing the spatial porosity distribution is shown in Figure 1. Grain boundary porosity dominates, though intragranular porosity was observed in biotite and feldspar grains. Due to drilling the core and sawing the sample, the disturbed zone occupied a depth of 1 mm from the surface.

## EXPERIMENTS

The experimental design for our rock-core column experiments is shown in Figure 2. Cores drilled perpendicular to the horizontal natural fracture of the Kuru Grey granite block were glued in series to form two longer rods, one (Core I) 74.5 cm long and the other (Core II) 68.5 cm long. In addition one short rod (Core III) of length about 28 cm was also employed in the experiments. Each rod, which had a diameter of 14 mm, was placed inside a plastic tube with an inner diameter of 15 mm, forming a flow channel in the 0.5 mm gap between the rod and the tube walls. The core-tube gap represents an artificial fracture. The volume of the flow channel in the 74.5 cm column was about 17 mL and that of the connecting tubing about 1.3 mL. Tracer experiments were performed using a peristaltic pump to control water flow rate. Water was fed into the columns at different flow rates of  $1\text{--}50 \mu\text{L}\cdot\text{min}^{-1}$ . A short tracer pulse ( $5 \mu\text{L}$ ) was injected into the water flow using an injection loop (Rheodyne) and the out flowing tracer was collected. A large number of tracer tests were performed using different tracers and different rock cores. Uranine, HTO,  $^{36}\text{Cl}$  and  $^{131}\text{I}$  were used as non-sorbing tracers,  $^{22}\text{Na}$  as a slightly sorbing tracer, and  $^{85}\text{Sr}$  as a sorbing tracer. The optical absorbance of uranine at 491 nm was measured by UV/VIS spectrophotometer, beta activities of HTO and  $^{36}\text{Cl}$  were determined by liquid scintillation counting and gamma activities of  $^{22}\text{Na}$ ,  $^{85}\text{Sr}$  and  $^{131}\text{I}$  were detected using a Wizard gamma counter. Synthetic granitic groundwater equilibrated with crushed rock material was used in all experiments.

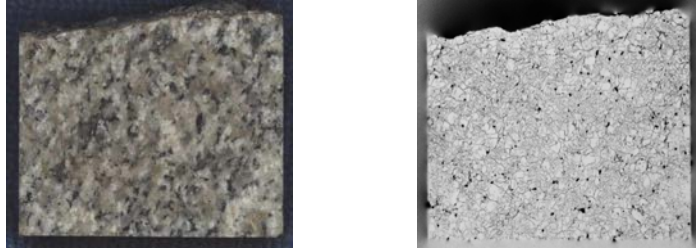


**Figure 1.** Photo micrograph of Kuru Grey granite and corresponding  $^{14}\text{C}$ -PMMA autoradiograph showing the spatial porosity distribution.



**Figure 2.** Photograph of the experimental set-up.

## RESULTS AND DISCUSSION

Several tracer tests were performed using uranine, HTO,  $^{36}\text{Cl}$  and  $^{131}\text{I}$  as non-sorbing,  $^{22}\text{Na}$  as a slightly sorbing and  $^{85}\text{Sr}$  as a sorbing tracer with injection flow rates  $1\text{--}50\ \mu\text{L}\cdot\text{min}^{-1}$ . All tracer tests were modelled to assess the influence of matrix diffusion in different tests. Solute mass flux through the transport channel was modelled by applying the assumption of a linear velocity profile and molecular diffusion. Coupling of the advection and diffusion processes was based on the model of generalised Taylor dispersion in the linear velocity profile. The model accounted for molecular diffusion both in the longitudinal direction and across the velocity profile. A detailed discussion of the problem and solution to the transport problem is given by Hautojärvi and Taivassalo [8].

Solute discharge at the end of the transport channel for the delta function release can be written as

$$j(t, t_w, u, R_a) = H(t - R_a t_w) \frac{u}{\sqrt{\pi}(t - R_a t_w)^{3/2}} e^{-\frac{u^2}{t - R_a t_w}}, \quad (1)$$

where parameter  $u$  determines the strength of the matrix diffusion,  $t_w$  is the groundwater transit time and  $R_a$  is the surface retardation coefficient.  $H$  is the cumulative distribution function. The matrix diffusion property ( $u$ ) is defined as

$$u = \varepsilon \sqrt{D_p R_p} \frac{W L}{Q} = \varepsilon \sqrt{D_p R_p} \frac{t_w}{2b}, \quad (2)$$

where  $t_w$  is the groundwater transit time,  $2b$  is the channel aperture,  $D_p$  is the matrix pore diffusivity,  $\varepsilon$  is the matrix porosity and  $R_p$  is the retardation coefficient in the matrix. The last part of the parameter  $u$ ,  $t_w/(2b)$ , is also presented as  $WL/Q$ . This parameter represents the coupling of the matrix diffusion to the flow field by ratio  $Q/W$ , i.e. flow rate per width and to the length of the channel  $L$ . Sorption was modelled as linear equilibrium sorption, both in the pore space of the rock matrix and on the outer surface of the core. Solute transport with matrix diffusion and sorption was calculated by integrating over the solute mass flux distribution according to Equation (3).

$$k(t) = \int_0^t j(t, t_w, U_t t_w, R_a) b(t_w) dt_w, \quad (3)$$

where  $b(t_w)$  is the solute mass flux distribution in the mobile pore space and  $j(t, t_w, U_t, R_a)$  is the corresponding sorption matrix diffusion breakthrough curve (Equation (1)).

This modelling work indicated that tests carried out with Core I had flow rates too high for clear indication of matrix diffusion. Tracer tests with the shortest core, Core III, were performed using a wide range of different tracers and flow rates. However, difficulties were faced in reproducing consistently the non-sorbing tracer breakthrough curves for different flow rates. Core II provided a consistent series of experimental results, and since it was longer than the Core III it emphasized the importance of matrix diffusion as a retention process. For this reason the main modelling effort focused on experiments performed using Core II. Breakthrough curves were modelled applying rock matrix characteristics and parameters estimated from previous experiments. The matrix pore diffusivity,  $D_p$ , was calculated from the rock porosity by applying Archie's law. The sorption properties of sodium were estimated from the values determined for Syry mica gneiss and unaltered tonalite using fracture and crushed rock columns [2]. The modelled breakthrough curves were calculated by assuming instantaneous release of the tracer (Dirac's delta function). The influence of tubing and other experimental equipment on the breakthrough curves was determined by performing tracer tests without the rock column. The modelled breakthrough curves for transport through the rock column were convoluted with a response function of the tubing before being compared with the measured experimental breakthrough curves.

Examples of the modelled and observed breakthrough curves for uranine and  $^{22}\text{Na}$  are presented in Figure 3. Especially interesting are the tailings of the low flow rate breakthrough curves. In the experimental breakthrough curves there appears to be clear differences in the tailings of uranine and  $^{22}\text{Na}$ . In the modelled curves this behaviour is explained well by the stronger matrix diffusion effect in  $^{22}\text{Na}$  breakthrough curves due to the sorption of  $^{22}\text{Na}$  in the pore space of the rock matrix.

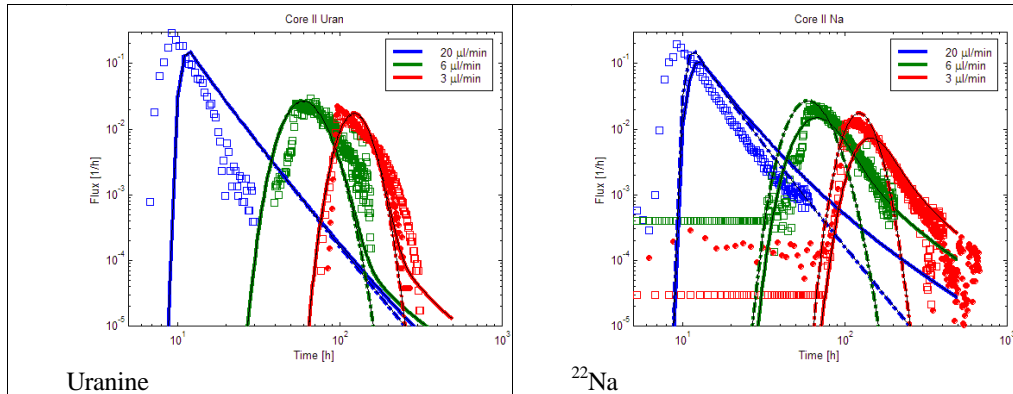


**Figure 3.** Modelled and measured breakthrough curves for uranine and  $^{22}\text{Na}$  through the Core II column. Flow rates were  $20 \mu\text{L}\cdot\text{min}^{-1}$  (left),  $6 \mu\text{L}\cdot\text{min}^{-1}$  (middle) and  $3 \mu\text{L}\cdot\text{min}^{-1}$  (right). Solid lines are modelled results for advection and matrix diffusion. Dotted lines are for the advection only.

The breakthrough curve for the highest flow rate was not well reproduced by the model. Reason for that was pump failure that resulted in the faster flow rate than set and used in model calculations. The breakthrough curve with the fastest flow rate,  $20 \mu\text{L}\cdot\text{min}^{-1}$ , was more advection–dispersion dominated than controlled by the matrix diffusion.

The matrix diffusion model applied in the modelling was based on the assumption of infinite rock matrix depth. The diameter of the borehole core was 14 mm and so it was necessary to estimate the possible influence of the limited thickness of the rock matrix to the breakthrough curves. One–dimensional calculations show that in the case of a non–sorbing tracer and limited rock matrix thickness, the breakthrough curve begins to deviate from the infinite rock matrix breakthrough curve at time  $t \sim R_a t_w + R_p L_z^2 / D_p$ , where  $t_w$  is the advective delay in the transport channel,  $R_a$  is the retardation coefficient for surface sorption,  $R_p$  is the retardation coefficient in the rock matrix,  $L_z$  is the thickness of the matrix, and  $D_p$  is the pore diffusivity. For a 5–mm layer of rock, the limited matrix thickness starts to influence a non–sorbing tracer breakthrough curve at around  $t \sim 240$  h; for moderately–sorbing  $^{22}\text{Na}$ , the breakthrough effect begins at  $t \sim 48\,000$  h. This means that it is possible that the uranine breakthrough curve shows some effects of the limitation in matrix thickness, but this is unlikely for  $^{22}\text{Na}$ . Finite thickness would result in reflective boundary conditions in which tracer transport approaches a steady state. Then all the molecules statistically experience the same velocities having equal transport time within a Gaussian distribution [2].

Scoping calculations were made to estimate how slow flow rates are needed to show the effects of matrix diffusion for non–sorbing tracers. The scoping calculations at decreased flow rates were based on the geometrical dimensions and evaluation of existing models and column tests. These calculations show that matrix diffusion begins to be observable for a non–sorbing tracer when the flow rate is around  $0.1 \mu\text{L}\cdot\text{min}^{-1}$  for the column experiment. The advection–governed tests were sensitive to transport porosity (i.e. transport to hydraulic aperture ratio x hydraulic volume), and the shape of the curve was sensitive to correlation length in the velocity profile. In scoping calculations the channel geometry, i.e. the effective channel width that influences the matrix diffusion, was based purely on geometrical considerations.

## CONCLUSIONS

Rock–core column experiments were performed to estimate the diffusion and sorption properties of Kuru Grey granite used in block–scale experiments. The experiments could be modelled by applying consistent parameterization and transport processes. The processes, advection–dispersion and matrix diffusion, were conceptualized with sufficient accuracy to replicate the experimental results. The results of the experiments provided evidence that it is possible to investigate matrix diffusion at the laboratory scale. The effects of matrix diffusion were demonstrated on the slightly sorbing tracer breakthrough curves. Based on scoping calculations matrix diffusion begins to be clearly observable for a non–sorbing tracer when the flow rate is below  $0.1 \mu\text{L}\cdot\text{min}^{-1}$ . The modelled experiment builds confidence on the model predictions of the solute retention in groundwater flow. The experimental results presented here cannot be transferred directly to the spatial and temporal scales that prevail in the underground repository. However, this knowledge and understanding of the transport and retention processes is transferable to different scales from laboratory to in–situ conditions.

## ACKNOWLEDGMENTS

This work is part of the Finnish Research Programme on Nuclear Waste Management (KYT2010) funded by the State Nuclear Waste Management Fund. The authors would like to thank Mr. Steward Makkonen-Craig for revising the language.

## REFERENCES

1. I. Neretnieks, T. E. Eriksen, and P. Tähtinen, *Water Resour. Res.* **18** (4), 849 (1982).
2. P. Hölttä, “Radionuclide migration in crystalline rock fractures–Laboratory study of matrix diffusion,” Doctoral Thesis, University of Helsinki. Report Series in Radiochemistry 20/2002, 55 p. + Appendices (2002).
3. P. Hölttä, A. Poteri, M. Hakanen and A. Hautojärvi, *Radiochimica Acta* **92**, 775 (2004).
4. A. Poteri and P. Hölttä, Technical Research Centre of Finland Research Report. VTT/PRO1/1008/05, 37 p (2005).
5. A. Poteri and P. Hölttä, Technical Research Centre of Finland Research Report. VTT-R-03919-06, 25 p. (2006).
6. K-H. Hellmuth, M. Siitari-Kauppi and A. Lindberg, *Journal of Contaminant Hydrology* **13**, 403 (1993).
7. M. Siitari-Kauppi, “Development of  $^{14}\text{C}$ -polymethylmethacrylate method for the characterisation of low porosity media,” Doctoral Thesis, University of Helsinki. Report Series in Radiochemistry 17/2002, 156 p (2002).
8. A. Hautojärvi and V. Taivassalo, Nuclear Waste Commission of Finnish Power Companies. Report YJT-94-24 (1994).